

# Flight Mechanics

## Aerodynamic and control analysis of J35 Draken

---



Nikolaos Koukis

## Contents

<b>1</b>	<b>Introduction</b>	<b>3</b>
<b>2</b>	<b>Performance Characteristics of J35 Draken</b>	<b>3</b>
2.1	Mathematical modelling	3
2.1.1	Static performance - Methodology	5
2.1.2	Minimum time problems set - Methodology	5
2.2	Static Performance	5
2.2.1	Excess Thrust	5
2.2.2	SEP Graph	6
2.3	Maximum altitude - Maximum Mach Number	7
2.4	Minimum time to climb	7
2.5	Computing $\gamma(t)$ - minimum time for Mach = 1.5 & h = 1.1km	8
2.6	Trajectory for maximum Mach number in minimum time	9
2.7	Trajectory for maximum altitude in minimum time	9
<b>3</b>	<b>Derivation of <math>C_l</math> rolling moment coefficient</b>	<b>10</b>
3.1	Simulation Considerations	11
3.2	Mathematical Modelling	11
3.3	Derivation of <i>damping-in-roll</i> derivative $C_{l_p}$	12
3.4	Derivation of the <i>Dihedral effect</i> $C_{l_\beta}$	13
<b>4</b>	<b>Stability and Control</b>	<b>16</b>
4.1	Equilibrium flight	16
4.1.1	Level Flight Trim Conditions	16
4.1.2	Center of gravity influence	17
4.1.3	Elevator per g	18
4.2	Linear stability analysis	19
4.3	Nonlinear simulation	20
4.3.1	Looping	22
4.3.2	Cobra Maneuver	23
4.3.3	The superstall	23
<b>5</b>	<b>Appendix</b>	<b>23</b>
	<b>References</b>	<b>28</b>

## List of Figures

2.1	Forces acting on the point mass system	4
2.2	Excess Thrust Graph	6
2.3	SEP Graph	7
2.4	Trajectory of the airplane to reach M = 1.5 & h = 11km	8
2.5	Velocity, height fuel consumption and $\gamma$ angle during the flight	8
2.6	Trajectory of the airplane to reach M = 1.76	9
2.7	Trajectory of the airplane to reach h = 16km	10
3.1	Picture of model during wind tunnel test	10
3.2	Examples of the data fitting procedure	12
3.3	Velocity - damping approximation curve	13
3.4	Fitting of polynomial curve into experimental data, for different $\alpha$ values	15
4.1	$\alpha, \delta_e, \delta_p$ for the trimmed Model	17
4.2	Elevator setting for different cg positions	18
4.3	Root Locus graph with regards to the airspeed	19
4.4	Simulation outcome for constant $\delta_e, \delta_p$	21
4.5	Nonlinear Simulation results for xcg = 10.3m	22
4.6	The looping maneuver	23

### Abstract

This work deals with various aspects of the *J35 Draken* aircraft performance. More specifically the report is divided into three main sections. In the first section we derive the excess thrust and envelope graphs and we also simulate for three optimization problems (reaching maximum altitude, maximum Mach number, etc) so that the ideal trajectory to fly with is found. In the second part the  $C_{lp}$ ,  $C_{l\beta}$  constants are calculated after the processing of experimental data. In the final part, we deal with various stability and control aspects of the aircraft, as well as with simulating a series of maneuvers (looping, cobra maneuver, etc).

The report is intended for the *Flight Mechanics* course offered by the School of Engineering Sciences in KTH. For the executed simulations, the *MATLAB* technical computing language was used.

**Keywords:** J35 Draken, Envelope limits, Trajectory optimization, Rolling moment coefficient, Linear stability, Control systems design.

## Nomenclature

$\alpha$	Angle of attack
$\beta$	Sideslip angle
$\epsilon$	Thrust angle
$\gamma$	Flight Path angle
$\rho$	Density of air
$\theta$	Angle of attitude
$C$	Damping coefficient of aircraft rolling motion
$C_l$	Rolling moment coefficient
$C_{l\beta}$	Dihedral Effect
$C_{lp}$	Damping in Roll Coefficient
$D$	Drag force
$h$	Aircraft altitude
$I_{xx}$	Rolling moment of inertia
$k$	Spring coefficient of aircraft rolling motion
$L$	Lift force
$l$	Rolling moment
$m$	Aircraft total mass
$p$	Roll angle derivative
$q$	Dynamical Pressure
$SEP$	Specific Excess Power
$T_{ex}$	Excess thrust
$u$	Projection of velocity on the x-axis of airplane (Body-fixed system)
$V$	Total Aircraft Velocity
$v$	Projection of velocity on the y-axis of airplane (Body-fixed system)
$w$	Projection of velocity on the w-axis of airplane (Body-fixed system)
$x_\epsilon$	Aircraft horizontal position displacement
$b$	Airplane Span

## S Airplane Surface Area

# 1 Introduction

The *SAAB J 35 Draken* was originally conceived as a replacement for the Swedish Air Force's venerable *J 29 Tunnan*, an aircraft that was the equivalent of the F-86 Sabre and MiG-15 in its capabilities, range, performance and load.

Regarding the aerodynamic design of the J35 Draken the two major options to chose from were swept wings and delta wings [1]. The question was quickly resolved by the initial studies which had called for the exploration of a swept wing configuration. In short order it was determined that in consideration of all other parameteres placed upon the design, the swept wing's aerodynamic drag at high Mach numbers was too high, and its configuration requirements dictated that the fuselage have insufficient volume for equipment, fuel and armament. The pure delta was also ruled out, however, as it suffered from center of gravity and center of pressure anomalies that were difficult to alleviate. A derivative, however, often referred to as *the double delta*, proved much more flexible.

In general the double delta was found to offer the attributes of:

- Reduced frontal area while permitting optimal wing area
- More favorable wing sweep angles on the center wing section
- Center of gravity and center of pressure being closer to each other
- More favorable area distribution
- Low supersonic drag
- Favorable low speed drag
- Strong and stiff fail safe structure
- Being able to place the air intakes farther forward

The plane's fuselage was a predictable tube with the engine mounted inside and the cockpit at the front and a vertical stabilizer attached to the tail [3]. The pointed nose cone contained a radar system and the air intakes for the engine were on either side of the cockpit at the forward point of the wing root. The double-delta began at the air intakes — for roughly two thirds of way toward the tips, the sweep back measured an incredibly sharp 80 degrees. This allowed the plane to achieve design speeds that were in excess of Mach 2.0. However, with such a sharp sweep, it was recognized that the plane would be seriously lacking in maneuverability. Thus, the last one third of the wings toward the tips carried a completely different sweep angle, much shallower at 60 degrees. This brought excellent maneuverability and enhanced control at low speeds.

## 2 Performance Characteristics of J35 Draken

### 2.1 Mathematical modelling

To determine the static performance characteristics of the aircraft as well as solve the minimum time problems set we need sufficient mathematical models to work with. For this part *the aircraft is modelled as a point mass system*. With this simplification in mind the forces acting on the airplane are given in fig. 2.1.

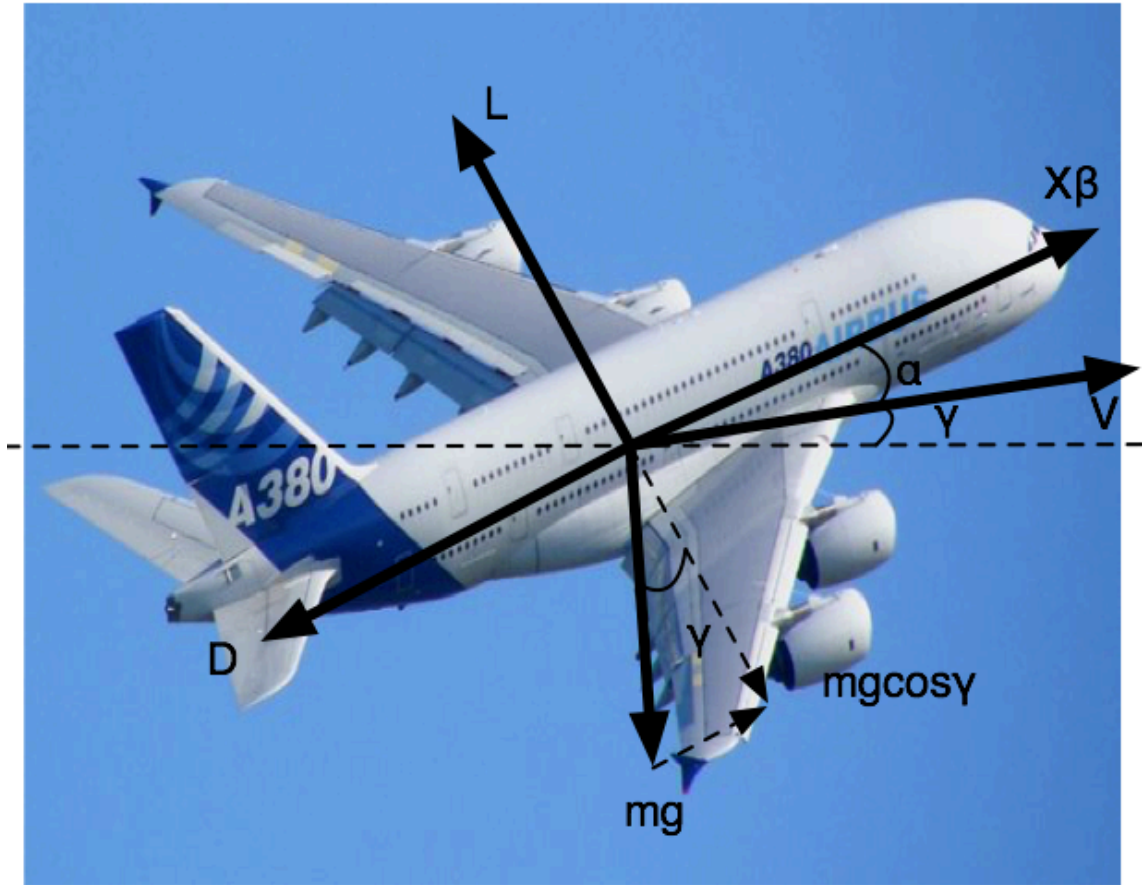


Figure 2.1: Forces acting on the point mass system

The set of differential equations governing the motion of the aircraft is stated below (Eq. 2.1-2.5):

$$m\dot{V} = T\cos(\alpha + \epsilon) - D - mg\sin\gamma \quad (2.1)$$

$$mV\dot{\gamma} = T\sin(\alpha + \epsilon) + L - mg\cos\gamma \quad (2.2)$$

$$\dot{h} = V\sin\gamma \quad (2.3)$$

$$\dot{x}_\epsilon = V\cos\gamma \quad (2.4)$$

$$\dot{n} = -b \quad (2.5)$$

To simplify the numerical solving procedure, we neglect the evolution of the horizontal displacement (Eq. 2.4). Instead, we calculate (in the end) the total distance covered by the aircraft during the simulation by integrating through the velocity values computed:

$$x_E(t) = \int_0^{t_f} V(t)\cos\gamma(t)dt \quad (2.6)$$

To simplify the model even further we assume that the acceleration perpendicular to the flight path is negligible ( $\dot{\gamma} = 0$ ) so that the system evolution is defined only by eq. 2.1, 2.3, 2.5:

$$m\dot{V} = T\cos(\alpha + \epsilon) - D - mg\sin\gamma$$

$$\dot{h} = V\sin\gamma$$

$$\dot{n} = -b$$

Final set of differential equations

### 2.1.1 Static performance - Methodology

To derive the excess thrust and SEP-Graphs we first *trim the aircraft* to obtain a flyable situation. This is done by solving eq. 2.2 for  $\dot{\gamma} = 0$  and finding a valid-for-flight  $\alpha$ . Then for given mach number and altitude compute the aerodynamic coefficients, the thrust the drag and the lift <sup>1</sup>

based on the given model, and finally we compute the excess thrust by computing the right-hand side of eq. 2.1. Finally we use the following equation for the computation of the Specific Excess Power.

$$SEP = \frac{T_{EX} V}{mg} \quad (2.7)$$

### 2.1.2 Minimum time problems set - Methodology

To find an optimum trajectory for the airplane to fly for different scenarios we first find a 'flyable' situation, as we mentioned previously, we find a valid  $\alpha$  for the initial mach number and altitude and then we *time integrate* the final set of differential equations derived, using  $\gamma$  as input to the system. So the task at hand using this strategy is to find the ideal  $\gamma$  input for achieving the defined goal each time.

## 2.2 Static Performance

### 2.2.1 Excess Thrust

In fig. 2.2 the Excess Thrust with regards to the Mach number is presented:

---

<sup>1</sup>The model for the lift force is the following:

$$L = C_L q_{dyn} S_{ref} \Rightarrow L = C_{La} (a_0 - c_{L0}) q_{dyn} S_{ref}$$

where, one can observe that  $C_L$  is not a non-dimensional quantity. That is due to the format of the aerodynamic data used for the simulation.

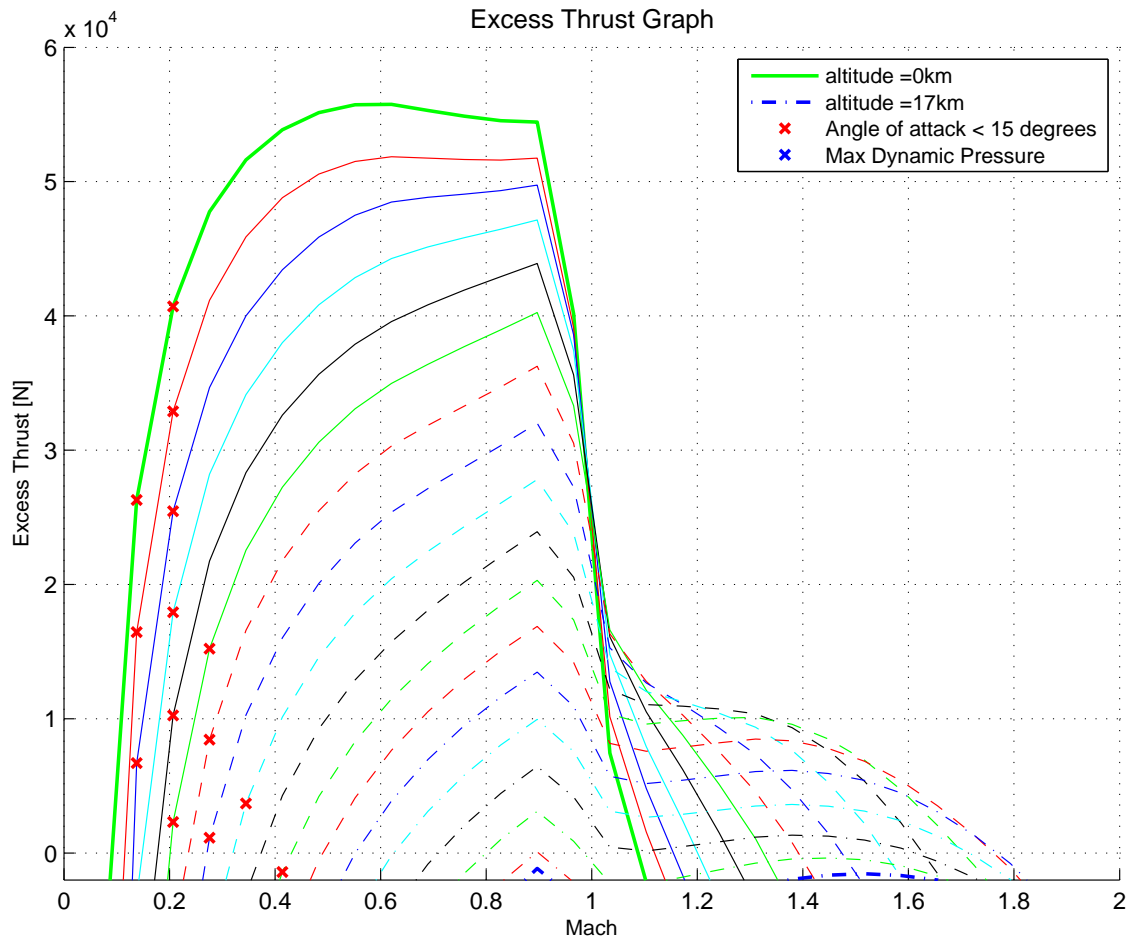


Figure 2.2: Excess Thrust Graph

Using the graph we can now determine the envelope limits corresponding to the dynamic pressure and the maximum angle of attack. These limits are shown in the diagram as red and blue Xs. We should note however that the dynamic pressure limits are not visible in 2.2, when presenting only the part of the diagram above the zero horizontal line.

### 2.2.2 SEP Graph

Having computed the Excess thrust of the aircraft model, we can now compute the Specific Excess Power and then form the Envelope graph of the Draken J35 by using eq. 2.7. The envelope graph is presented in fig. 2.3.

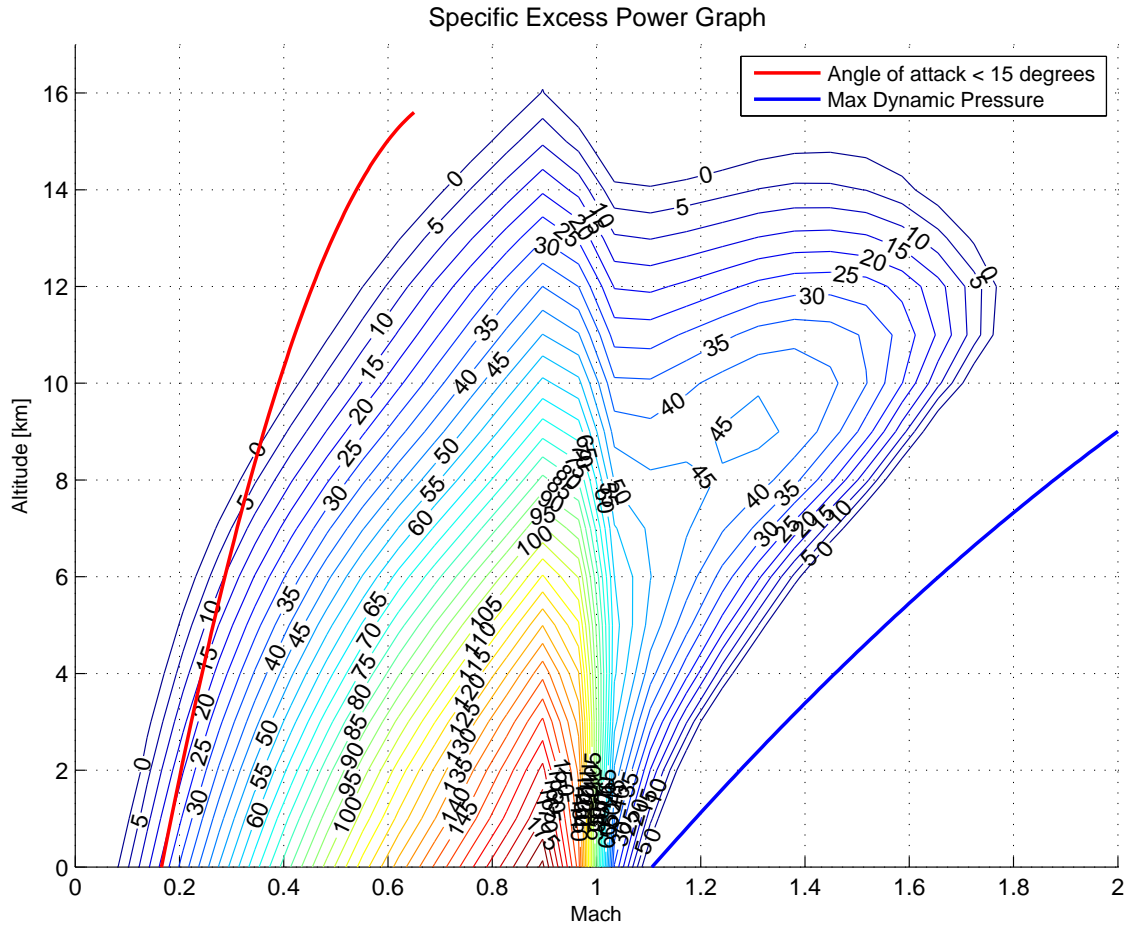


Figure 2.3: SEP Graph

Graph 2.3 shows the contours of same Excess Power with regards to the altitude of the airplane as well as the Mach number thus the velocity of the airplane.

Using this graph we can also determine the envelope limits corresponding to the maximum angle of attack ( $15^\circ$ ) and the maximum dynamic pressure corresponding to  $1350 \text{ km/h}$  at sea level which is  $8.6133e^{+04} \text{ Pa}$ .

### 2.3 Maximum altitude - Maximum Mach Number

The maximum altitude and the maximum Mach Number at which the aircraft can fly level can be determined using 2.3:

- Max. Altitude: 16 km
- Max Mach: 1.76

### 2.4 Minimum time to climb

The current task is to find using trial and error methods, the minimum time to reach certain goals. To investigate the situation more thoroughly in each try we plot the total energy lines as well as plots for the fuel consumption the speed of the airplane the height and the  $\gamma$  angle.



## 2.5 Computing $\gamma(t)$ - minimum time for Mach = 1.5 & h = 11km

The feasible solution to the above challenge is shown in 2.4. 2.5 is also presented to show the changes of the different properties during the time of flight

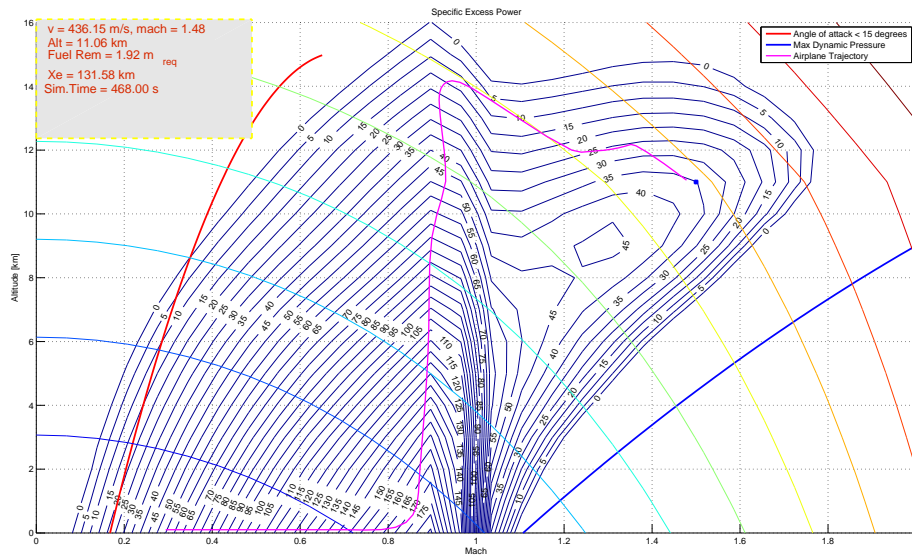


Figure 2.4: Trajectory of the airplane to reach M = 1.5 & h = 11km

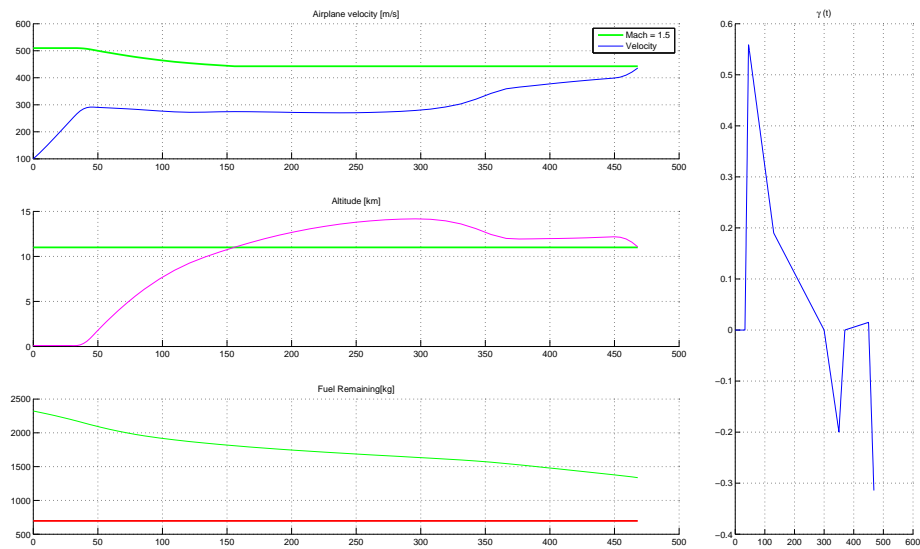


Figure 2.5: Velocity, height fuel consumption and  $\gamma$  angle during the flight

The strategy of the climb is first to climb to higher altitude than needed and then dive into the supersonic area "with the same slope as an energy line" to lose the least amount of energy during the maneuver. As we see the aircraft reaches the goal after 468 seconds which is acceptable both in terms of fuel consumption and afterburner time of use.

## 2.6 Trajectory for maximum Mach number in minimum time

To reach the maximum Mach number given by the SEP graph we use the same tactic as in 2.5. The diagram 2.6 corresponding to the flight are also given below:

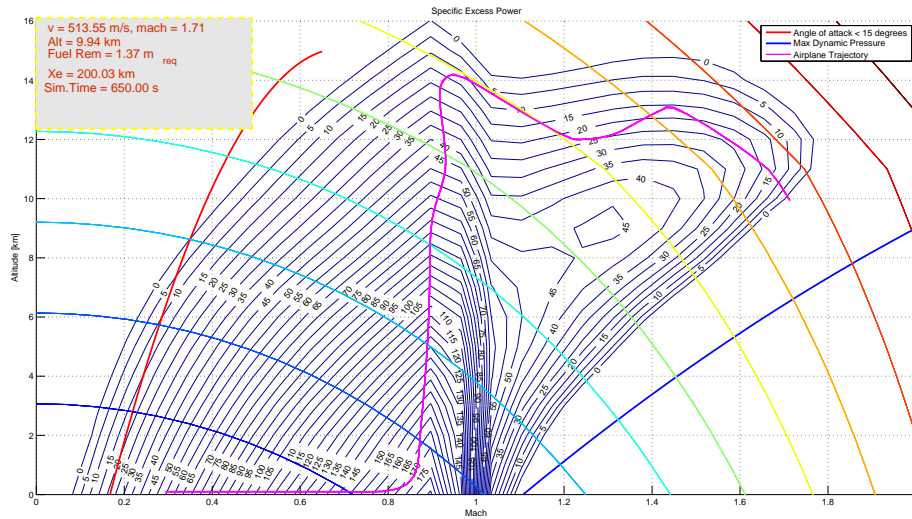


Figure 2.6: Trajectory of the airplane to reach  $M = 1.76$

## 2.7 Trajectory for maximum altitude in minimum time

The diagram for reaching the maximum altitude is given in 2.7. It is visible that the trajectory is not the best possible as the aircraft reaches a maximum of 15.4 km instead of the actual goal which is 16 km.

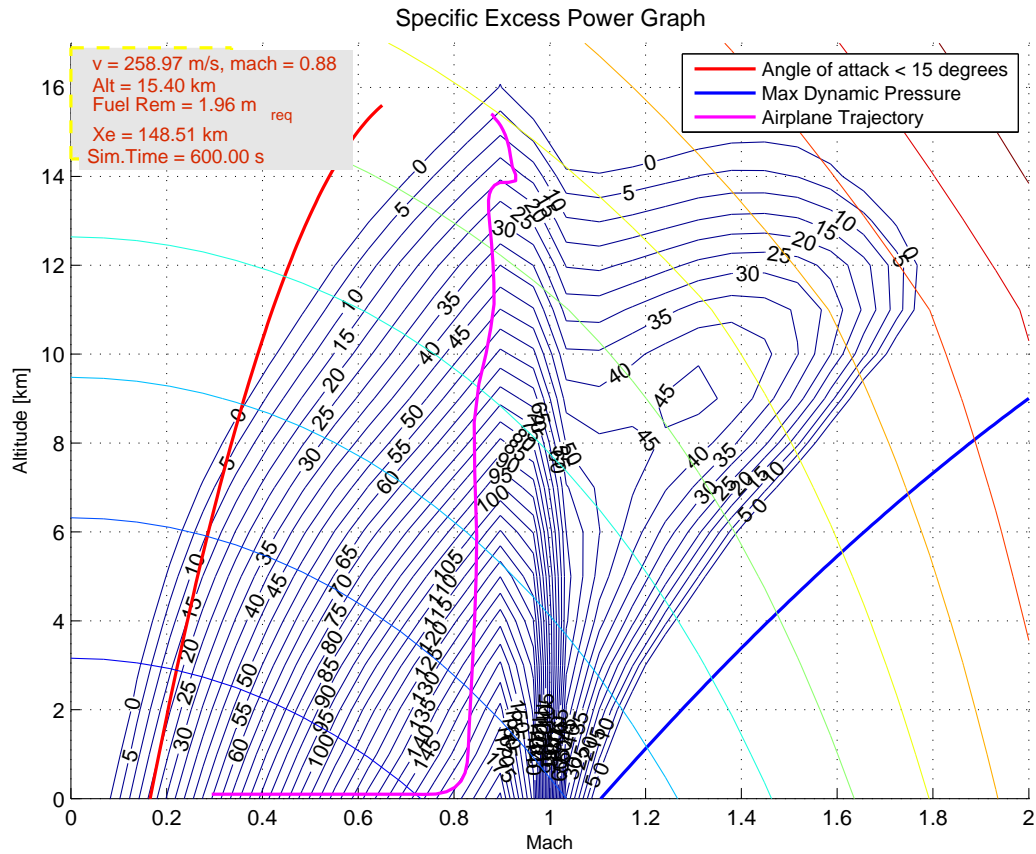


Figure 2.7: Trajectory of the airplane to reach  $h = 16\text{km}$

### 3 Derivation of $C_l$ rolling moment coefficient

In this part of the project the rolling moment coefficient of the J35 Draken is to be calculated. For the simulation, the model of fig.3.1 was used:



Figure 3.1: Picture of model during wind tunnel test

### 3.1 Simulation Considerations

The following can be stated when comparing the J35 Draken aircraft with the wind tunnel model used(fig. 3.1)

- Apparently the major difference is the *absence of the fin*. This fact eventually caused considerable divergence between the values computed during the simulation and the data extracted from Draken data diagrams provided.
- The wind tunnel model scale was 1:14.7 except for the bodywidth and noselength.

### 3.2 Mathematical Modelling

To proceed with the analysis and the computation of  $C_{lp}$ ,  $C_{l\beta}$  parameters, a valid mathematical model needs to be derived first. If We implement the Newton's second law for the rolling movement we can derive equation 3.1.

$$\Sigma T = I_{xx}\ddot{\phi} \Rightarrow l - C\dot{\phi} - k\phi = I_{xx}\ddot{\phi}, \quad (3.1)$$

where  $C\dot{\phi}$  is the moment exerted due to the (mechanical) damping and  $k\phi$  is the moment due to the (mechanical) spring stiffness of the device holding the airplane during the simulation. For the calculation of the rolling moment the following equations can be used:

$$l = C_l q b S \quad (3.2)$$

$$C_l = C_{lp} \frac{pb}{2u} + C_{l\beta} \beta \quad (3.3)$$

$$p = \dot{\phi}$$

$$q = \frac{1}{2} \rho v^2$$

A sufficient model of calculating  $C_l$  - the rolling moment coefficient - is given in equation 3.3. According to this,  $C_l$  is a function of  $C_{lp}$  the *damping-in-roll* coefficient and  $C_{l\beta}$  the dihedral effect.  $C_{lp}$  expresses the resistance of the airplane to rolling [2], while  $C_{l\beta}$  expresses the change in rolling moment coefficient per degree of change in the sideslip angle  $\beta$ . A sufficient relation to calculating  $\beta$  can be the following:

$$\beta = \alpha \phi \quad (3.4)$$

If we now substitute the expression of rolling moment 3.2 into the initial equation 3.1, and move all the  $\phi$ ,  $\dot{\phi}$  terms to the other side of the equation we can end up with the following second order differential equation:

$$I_{xx}\ddot{\phi} + \dot{\phi}(C_{mech} - \frac{C_{lp} S b^2 q}{2u}) + (k - C_{l\beta} a q b S) \phi = 0 \quad (3.5)$$

The analytical solution of 3.5 for the general case of complex roots (which is what we expect due to the oscillatory behavior of the model movement) is the following:

$$\phi = c_1 e^{\alpha' x} \cos(\beta' x) + c_2 e^{\alpha' x} \sin(\beta' x) \quad (3.6)$$

$$\begin{aligned} \alpha' &= -\frac{\beta}{2\alpha} \\ \beta' &= \frac{\sqrt{4ac - b^2}}{2a} \end{aligned} \quad (3.7)$$

where  $\alpha, \beta, c$  are the coefficients of 3.5 respectively:

$$\alpha = I_{xx} \quad (3.8)$$

$$\beta = C_{mech} - \frac{C_{lp} S b^2 q}{2u} \quad (3.9)$$

$$c = k - C_{l\beta} a q b S \quad (3.10)$$

To get the analytical solution of the roll rate  $\dot{\phi}$  we take the derivative of 3.6:

$$\begin{aligned} \dot{\phi} &= (-C_1 \beta' \sin(\beta' x) + C_2 \beta' \cos(\beta' x)) e^{\alpha' x} = \\ &= \beta' (-C_1 + C_2) e^{\alpha' x} (\sin(\beta' x) + \cos(\beta' x)) = \\ &\Rightarrow \{A = \beta' (-C_1 + C_2)\} \Rightarrow \\ \dot{\phi} &= A e^{\alpha' x} (\sin(\beta' x) + \cos(\beta' x)) = \\ &\Rightarrow \{a \sin(\theta) + b \cos(\theta) = R \sin(\theta \pm \alpha)\} \Rightarrow \\ \dot{\phi} &= A e^{\alpha' x} (\sin(\beta' x + \Theta)) \end{aligned} \quad (3.11)$$

### 3.3 Derivation of *damping-in-roll* derivative $C_{lp}$

To derive the  $C_{lp}$  parameter, we first need to extract information out of the experimental data gathered. The oscillation of the rolling motion can be modelled as a decaying sinusoidal function of time. Therefore we can fit an exponential sinusoidal function of the form 3.11 in the data and estimate each parameter by using the least squares method.

The data fit procedure uses the Fourier transform to extract the basic frequency as well as the least squares method. Figures 3.2a, 3.2b show some examples of the data fits that demonstrate the efficiency of the approximation algorithm used.

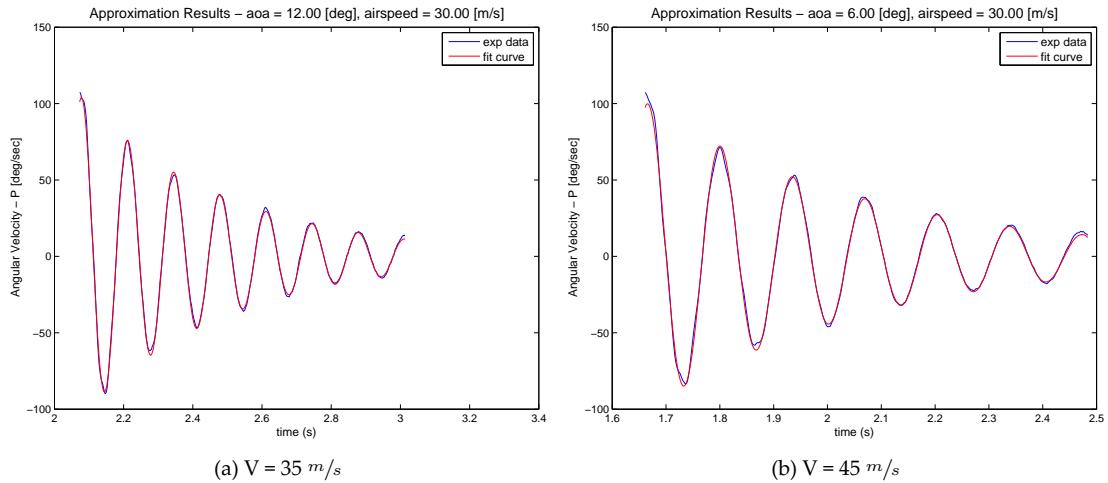


Figure 3.2: Examples of the data fitting procedure

To derive only the value of the  $C_{lp}$  parameter we have to take into account *only the data for  $\alpha = 0$* , because otherwise  $C_{l\beta}$  starts to play a role in the behavior of the oscillation (see eq. 3.5).

To extract the maximum amount of data and be as accurate as possible we *process all the  $\alpha = 0$  measurements taken during the laboratory sessions.*<sup>2</sup>

The procedure can be summarised in the next steps:

1. Calculation of  $C_{mech}, I_{xx}$ <sup>3</sup> using one of the  $\alpha = 0, V = 0$  measurements available.

<sup>2</sup>The reader is encouraged to refer to stiff.m of the code part for the actual implementation

<sup>3</sup>I know that  $I_{xx} = \sqrt{\frac{k}{\omega^2}}$  where k has already been determined experimentally.

2. Approximation of the  $n$ - $v$ <sup>4</sup> curve by using a wide range of velocities to calculate  $n$ -values and by using the least squares method.
3. Calculation of the  $n$ - $v$  curve slope from which knowing every other quantity I can extract an estimation of the  $C_{lp}$  value.

Using this strategy we can now derive the approximation curve of the  $n$ - $v$  points:

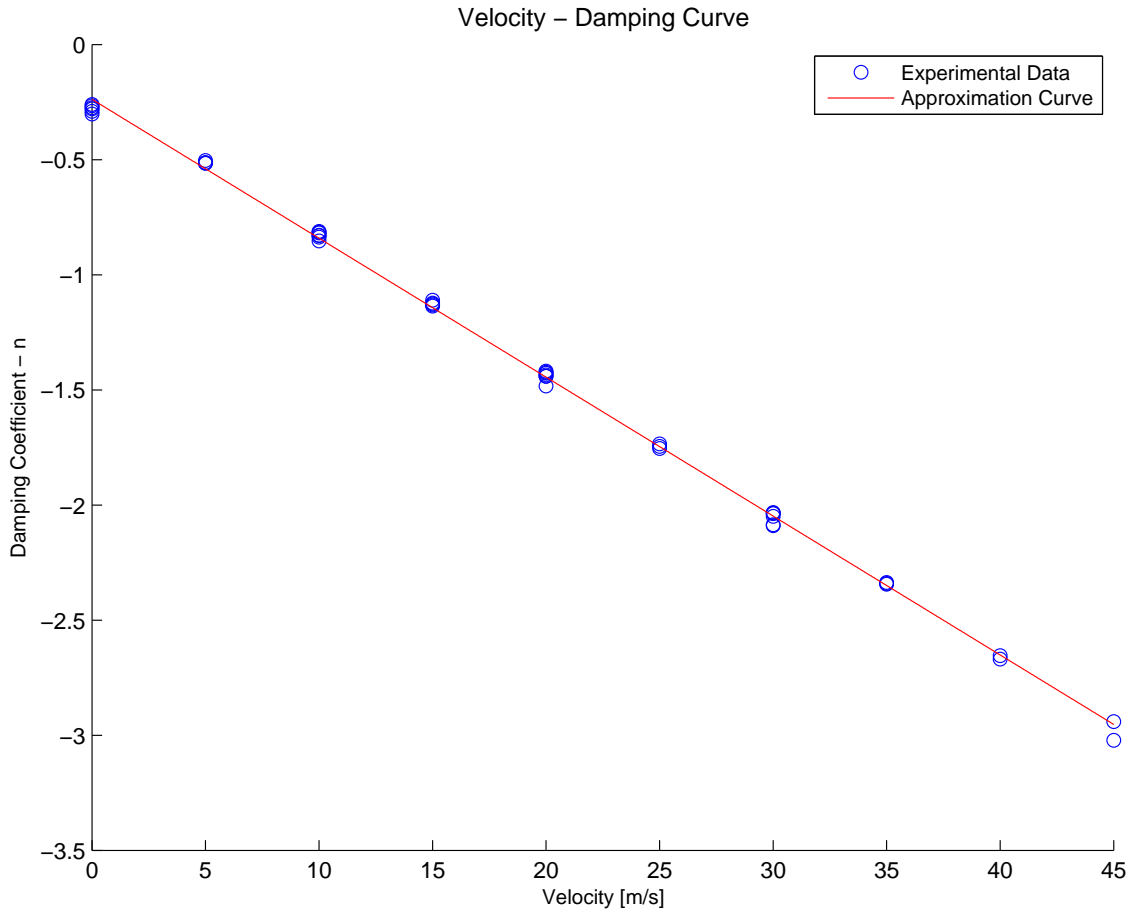


Figure 3.3: Velocity - damping approximation curve

From the above graph and using the methodology described in the previous steps we can now conclude to the value of  $C_{lp}$ :

$$C_{lp} \simeq -0.190 \quad (3.12)$$

Since this value is (strictly) negative and is close to the data given for the real aircraft (for  $\alpha = 0$ ), We can conclude that it is a logical estimation of the damping-in-roll coefficient.

### 3.4 Derivation of the *Dihedral effect* $C_{l\beta}$

We use the same strategy as in the derivation of  $C_{lp}$  to find a formula for calculating  $C_{l\beta}$ .  $C_{l\beta}$  appears only in the formula of  $\beta'$  (see eq. 3.6) which corresponds to the natural frequency of the aircraft oscillation. Executing the necessary computations, we can find an expression for the calculation of  $C_{l\beta}$ .

<sup>4</sup> $n$  is the damping coefficient, equivalent to  $\beta'$  of eq. 3.11

$$\begin{aligned}
 \omega_n &= \beta' = \frac{\sqrt{4\alpha c - \beta^2}}{2\alpha} \Rightarrow \\
 \omega_n^2 &= \frac{4\alpha c - \beta^2}{4\alpha^2} \Rightarrow \\
 &\Rightarrow \{\text{Substituting quantities from eq. 3.8-3.10}\} \Rightarrow \\
 \omega_n^2 &= -\left(\frac{C_{l\beta}\alpha\rho bS}{2I_{xx}} + \frac{C_{lp}^2\rho S^2b^4\rho^2}{64I_{xx}^2}\right)V^2 + \left(\frac{C_{mech}C_{lp}Sb^2\rho}{8I_{xx}^2}\right)V + (4I_{xx}k - C_{mech}^2) \quad (3.13)
 \end{aligned}$$

If we now fit the experimental data ( $V, \omega_n^2$ ) into a quadratic polynomial model of the form  $ax^2 + bx + c$  using the least squares method and extract the coefficients  $a, b, c$  we can find an analytical formula for  $C_{l\beta}$ . So taking this into account and knowing that  $C_{l\beta}$  appears in the expression of the first coefficient of the  $V - \omega_n^2$  curve, we end up with the following expression:

$$C_{l\beta} = -\left(\frac{2I_{xx} \times \text{coeff}(1)}{\alpha\rho bS} + \frac{C_{lp}^2 S b^3 I_{xx}}{32I_{xx}^2 \alpha b}\right) \quad (3.14)$$

As we can see from eq 3.14  $C_{l\beta}$  is a function of the first coefficient of the fitting curve ( $\text{coeff}(1)$ ), of  $C_{lp}$  which was previously calculated, and of  $\alpha$ . To proceed to the actual calculation, we fit quadratic polynomial curves over the  $V - \omega^2$  pairs for each value of  $\alpha$  and therefore calculate the  $C_{l\beta}$  values.<sup>5</sup>

Having executed the above procedure we end up with the following graphs for different  $\alpha$  angles<sup>6</sup>

<sup>5</sup>We consider only the values of  $\alpha$  for which sufficient experimental data has been gathered. See `stiff.m` for the actual implementation

<sup>6</sup>Some basic filtering was needed for the gathered experimental points. More specifically points that were outside the range of 3

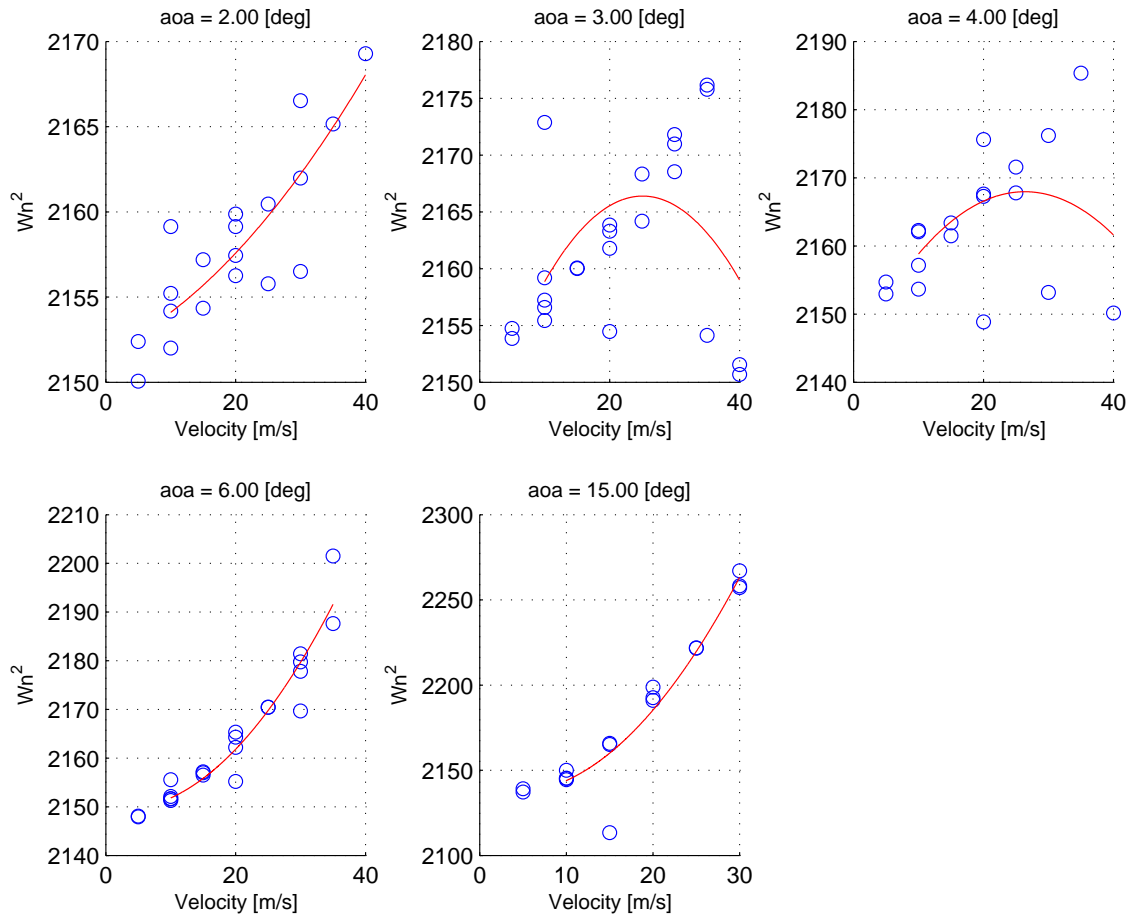


Figure 3.4: Fitting of polynomial curve into experimental data, for different  $\alpha$  values

If we now extract  $C_{l\beta}$  using eq. 3.14 we end up with the following values:

- $\alpha = 2^\circ \rightarrow \beta = -0.0026$
- $\alpha = 3^\circ \rightarrow \beta = 0.0048$
- $\alpha = 4^\circ \rightarrow \beta = 0.0037$
- $\alpha = 6^\circ \rightarrow \beta = -0.0037$
- $\alpha = 15^\circ \rightarrow \beta = -0.0063$



## 4 Stability and Control

### 4.1 Equilibrium flight

For the following analysis the following set of kinematic and dynamical equations describes the motion of the aircraft sufficiently:

$$X - mg\sin\theta = m(\dot{u}^E + qw^E - rv^E) \quad (4.1)$$

$$Y + mg\cos\theta\sin\phi = m(\dot{v}^E + ru^E - pw^E) \quad (4.2)$$

$$Z + mg\cos\theta\cos\phi = m(\dot{w}^E + pv^E - qu^E) \quad (4.3)$$

$$L = I_x\dot{p} - I_{zx}\dot{r} + qr(I_z - I_y) - I_{zx}pq + qh'_z - rh'_y \quad (4.4)$$

$$M = I_y\dot{q} + rp(I_x - I_z) - I_{zx}(p^2 - r^2) + rh'_x - ph'_z \quad (4.5)$$

$$N = I_z\dot{r} - I_{zx}\dot{p} + pq(I_y - I_x) + I_{zx}qr + ph'_y - qh'_x \quad (4.6)$$

$$p = \dot{\phi} - \dot{\psi}\sin\theta \quad (4.7)$$

$$q = \dot{\theta}\cos\phi + \dot{\psi}\cos\theta\sin\phi \quad (4.8)$$

$$r = \dot{\psi}\cos\theta\cos\phi - \dot{\theta}\sin\phi \quad (4.9)$$

$$\dot{\phi} = p + (q\sin\phi + r\cos\phi)\tan\theta \quad (4.10)$$

$$\dot{\theta} = q\cos\phi - r\sin\phi \quad (4.11)$$

$$\dot{\psi} = (q\sin\phi + r\cos\phi)\sec\theta \quad (4.12)$$

$$\begin{aligned} \dot{x}_E &= u^E\cos\theta\cos\psi + u^E(\sin\phi\sin\theta\cos\psi - \cos\phi\sin\psi) + \\ &+ w^E(\cos\phi\sin\theta\cos\psi - \sin\phi\sin\psi) \end{aligned} \quad (4.13)$$

$$\begin{aligned} \dot{y}_E &= v^E\cos\theta\sin\psi + v^E(\sin\phi\sin\theta\sin\psi + \cos\phi\cos\psi) + \\ &+ w^E(\cos\phi\sin\theta\sin\psi - \sin\phi\cos\psi) \end{aligned} \quad (4.14)$$

$$\dot{z}_E = -u^E\sin\theta + v^E\sin\phi\cos\theta + w^E\cos\phi\cos\theta \quad (4.15)$$

$$u^E = u + W_x \quad (4.16)$$

$$v^E = v + W_y \quad (4.17)$$

$$w^E = w + W_z \quad (4.18)$$

The above equations contain the following assumptions:

- The airplane is a rigid body, which may have attached to it any number of rigid spinning rotors.
- $C_{xz}$  is a plane of mirror symmetry.
- The axes of any spinning rotors are fixed in direction relative to the body axes, and the rotors have constant angular speed relative to the body axes.

#### 4.1.1 Level Flight Trim Conditions

As in the 1st part of the report, we have to first find a flyable situation for the aircraft model. This is done by setting as many states of the above equations to zero. Equations 4.1,??,4.15 give 3 nonlinear algebraic equations. We also choose to set  $\dot{M} = 0$  and also know the formula for the velocity magnitude,  $V = u^2 + v^2$  since  $w = 0$ .

So we end up with the following set of equations which we solve to compute the trimmed state.

$$X - mg \sin \theta = 0 \quad (4.19)$$

$$Z + mg \cos \theta = 0 \quad (4.20)$$

$$-u^E \sin \theta + w^E \cos \theta = 0 \quad (4.21)$$

$$\dot{M} = 0 \quad (4.22)$$

$$V^2 = u^2 + v^2 \quad (4.23)$$

Set of nonlinear equations for trimmed state

After finding an initial flyable situation, we linearise initial set of differential equations so that we end up with a system of the form:

$$\dot{\underline{x}} = \underline{J} \underline{\Delta x} + \underline{B} \underline{\Delta c}$$

$$\underline{y} = \underline{C} \underline{\Delta x}$$

where for negligible input the differential equations are trimmed down to the  $\dot{\underline{x}} = \underline{J} \underline{\Delta x}$  linear system.

Executing this procedure for mach numbers in the range of 0.1-0.7 and altitudes 0, 5000, 10000m we obtain the following graphs for  $\alpha$ ,  $\delta_e$ ,  $\delta_p$ :

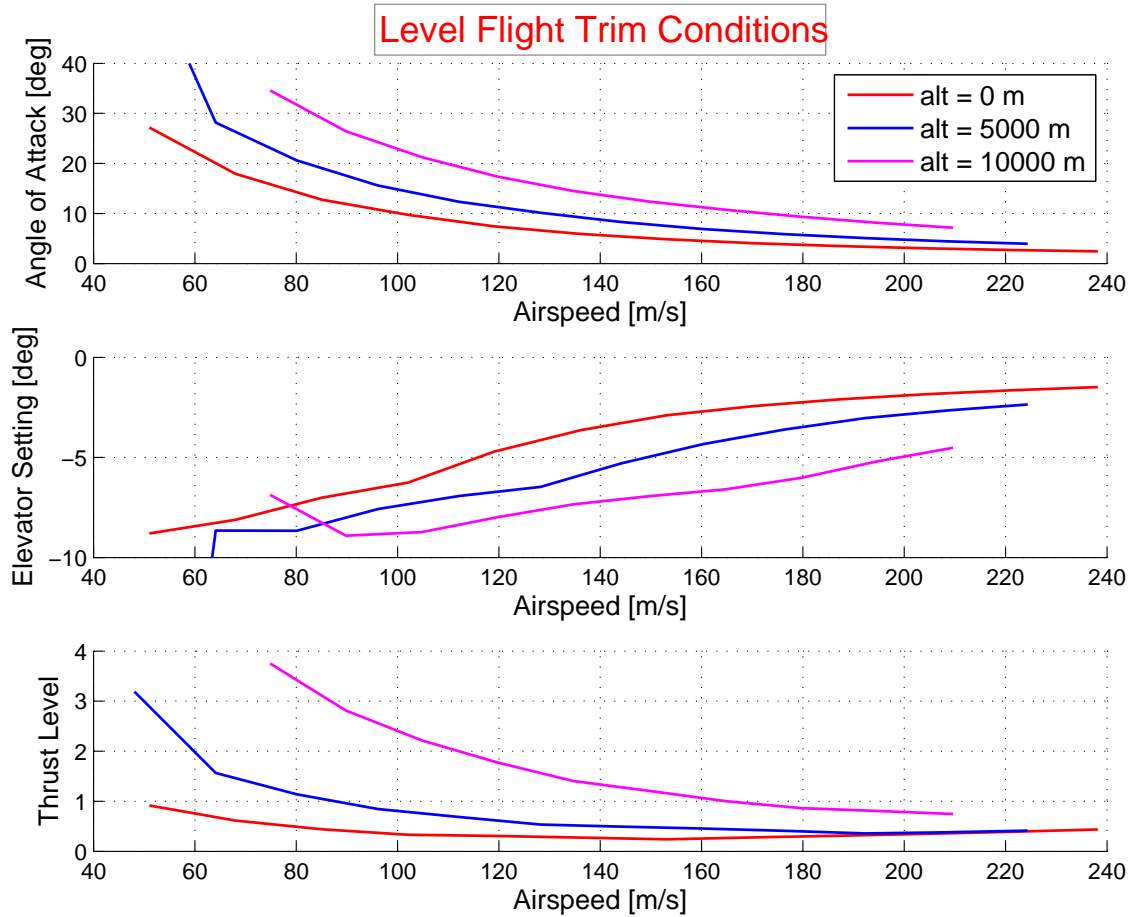


Figure 4.1:  $\alpha, \delta_e, \delta_p$  for the trimmed Model

#### 4.1.2 Center of gravity influence

To investigate the influence of the center of gravity (x<sub>cg</sub>) on the elevator angle we plot the equilibrium elevator as a function of the airspeed for an altitude of 5000m for two different x<sub>cg</sub> values (10.0, 10.3)m. The result is shown in fig 4.2.

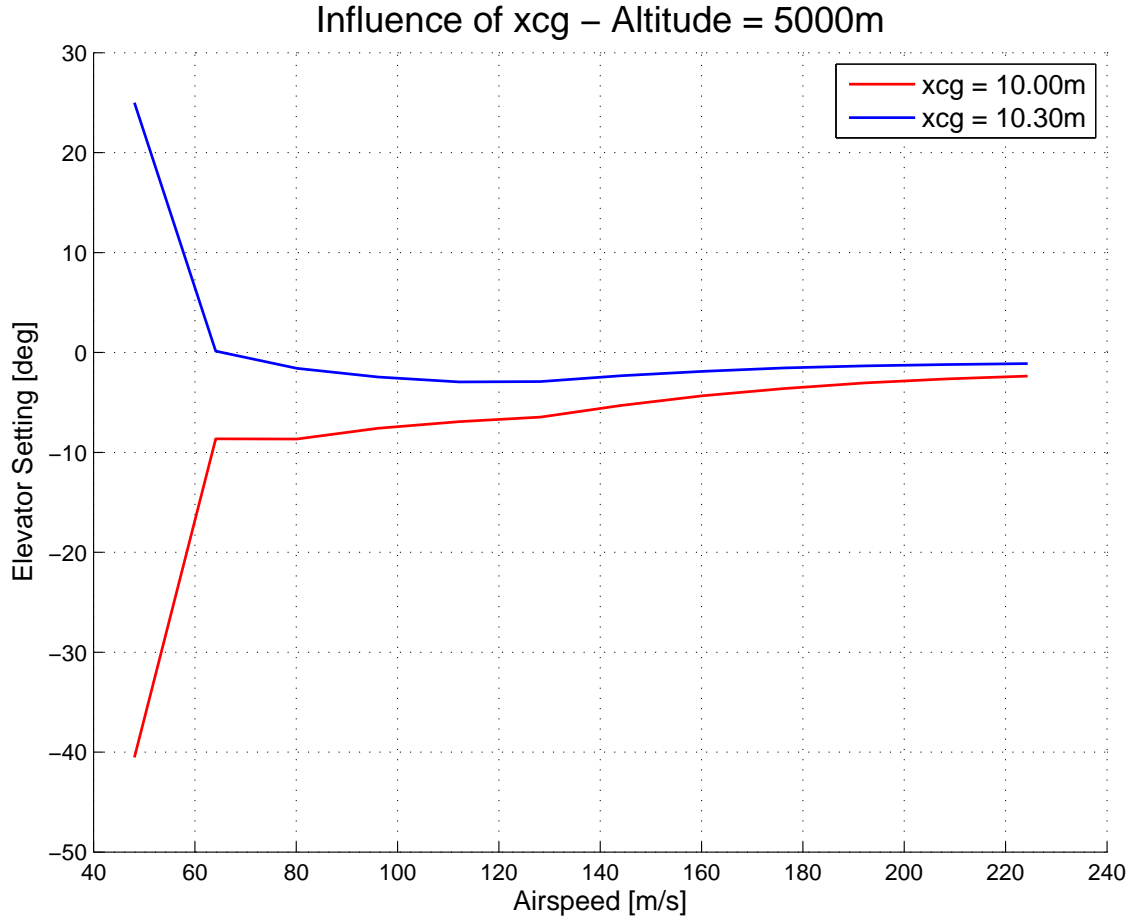


Figure 4.2: Elevator setting for different cg positions

As we can see the sign of the setting changes to positive<sup>7</sup> at low airspeed. This is because the center of gravity has moved further away from the tip of the aircraft comparing to the aerodynamic center, so a torque emerges pushing the nose of the aircraft upwards. So in order for the pitch-motion to be stable the elevator has to be positive as it is when  $x_{cg} = 10.3m$ . So we can conclude that since the elevator setting is positive for a wide range of airspeeds,  $x_{cg} = 10.3m$  is not allowed position for the aircraft.

#### 4.1.3 Elevator per g

The *Elevator per g* can be computed using the following formula:

$$Elevator_{per_g} = \frac{\Delta \delta e}{n - 1} \quad (4.24)$$

In order to find it, we hold the velocity constant and the the thrust level zero, for certain altitude and we implement a step input to the elevator. We then take measure the difference in the load factor and therefore compute the elevator per g from eq. 4.24. We end up with the followign results which show that the epg goes down as the altitude increases.<sup>8</sup>:

- $Altitude = 0m \rightarrow Epg = 16.660$
- $Altitude = 5000m \rightarrow Epg = 5.892$
- $Altitude = 10000m \rightarrow Epg = 1.792$

<sup>7</sup>The elevator setting is defined as positive when the elevator goes down.

<sup>8</sup>The results are also handed in as logfiles, see `elevator_per_g.log`

## 4.2 Linear stability analysis

In order to investigate the linear stability of the aircraft we have to perform an eigenvalue analysis for the Jacobian matrix computed during the trim problem

We compute the eigenvalues for altitudes 0, 5000, 10000m and for mach numbers in the range of 0.1 - 0.7. We then plot the root locus graphs of the eigenvalues with airspeed as a parameter.

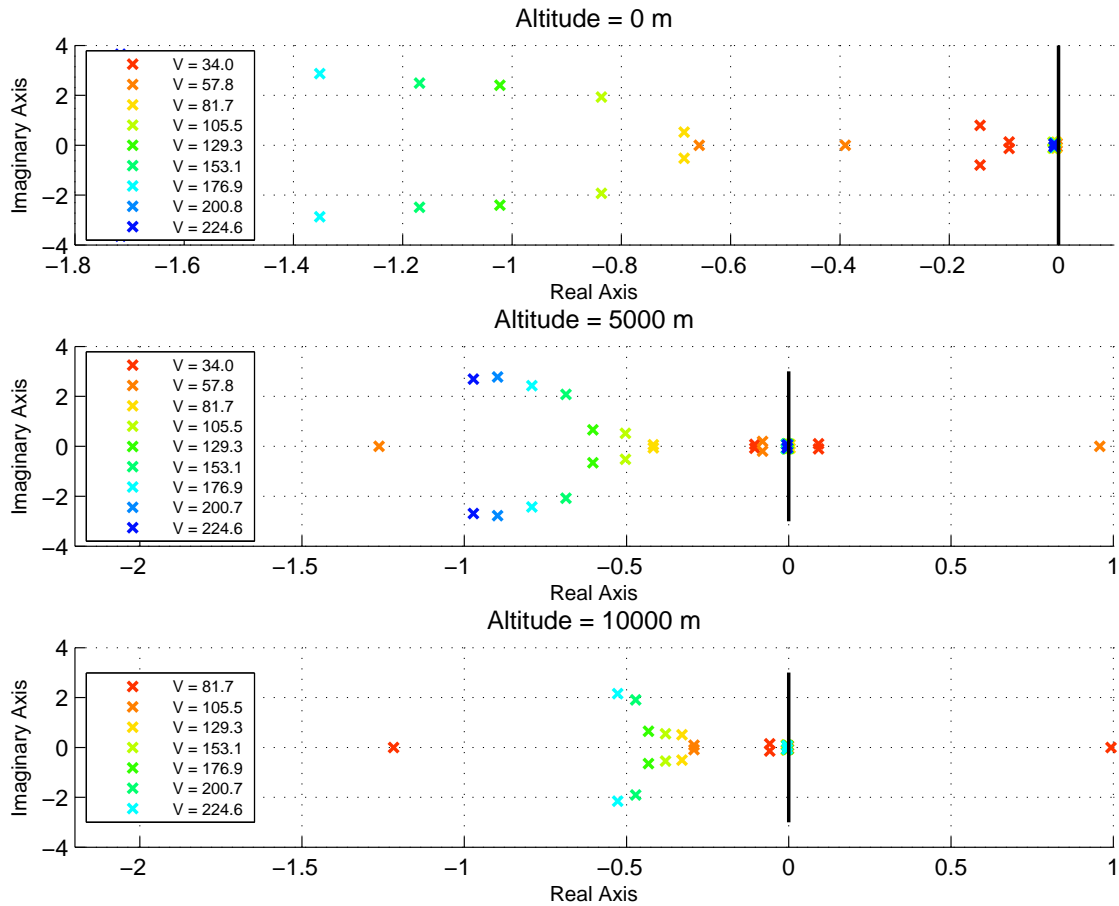


Figure 4.3: Root Locus graph with regards to the airspeed

From fig. 4.3 we can see that the linearised model *is not stable* for low airspeeds at altitude increases. More specifically, at  $h = 5000m$ , the system is unstable for  $V = 34m/s$  and  $V = 57.8m/s$  and it becomes stable as the airspeed increases to  $81.7m/s$ . For  $h = 10000m$  on the other hand, we could not even reach an equilibrium trim state for  $V \leq 81.7ms$ .

In particular, because we are interested in the stability of the longitudinal movement we investigate the behavior of a submatrix of  $J$  that corresponds to the longitudinal equations [2].

$$J' = J(\Delta\dot{u}, \dot{w}, \dot{q}, \Delta\dot{\theta}) \quad (4.25)$$

For the stability analysis we compute the following based on  $J'$ :

- Eigenvalues  $\lambda$
- Eigenvectors  $v$
- Oscillation frequencies  $f$
- Time to half/double

To compute the eigenvalues and eigenvectors, we implement the following methodology:

$$\begin{aligned} J'v &= \lambda v \Rightarrow \\ (J' - \lambda I)v &= 0 \Rightarrow \\ |J' - \lambda I| &= 0 \end{aligned} \quad (4.26)$$

Using eq (4.26) we can calculate the eigenvalues of the matrix by solving the polynomial equation. Then to compute the corresponding eigenvector we substitute each  $\lambda$  calculated in the initial equation:

$$(J' - \lambda_i I)v_i = 0, \text{ for } i = 1, \dots, N, \quad (4.27)$$

where  $N$  is the total number of eigenvalues

We also know that since the eigenvalues computed are of the form  $n \pm i\omega$ , the frequency of each oscillation mode can be computed directly from the eigenvalues:

$$f = \frac{\omega}{2\pi} \quad (4.28)$$

The time to double/half can also be obtained using the following formula [2].

$$t_{double} = t_{half} = \frac{\log_e 2}{|n|} \quad (4.29)$$

Finally having computed the eigenvalues and the corresponding eigenvectors, the oscillation modes can be computed using the following expression:

$$\mathbf{X} = \mathbf{X}_0 e^{\lambda t} \quad (4.30)$$

The results of the eigenvalue analysis are presented in the appendix of the report and are also handed in as logfiles.

### 4.3 Nonlinear simulation

We now simulate the behavior of the aircraft when executing each one of the following 3 situations:

- Looping
- Cobra Manuever
- Superstall

We first run the simulation for 300 seconds with fixed inputs for the elevator and the thrust level.

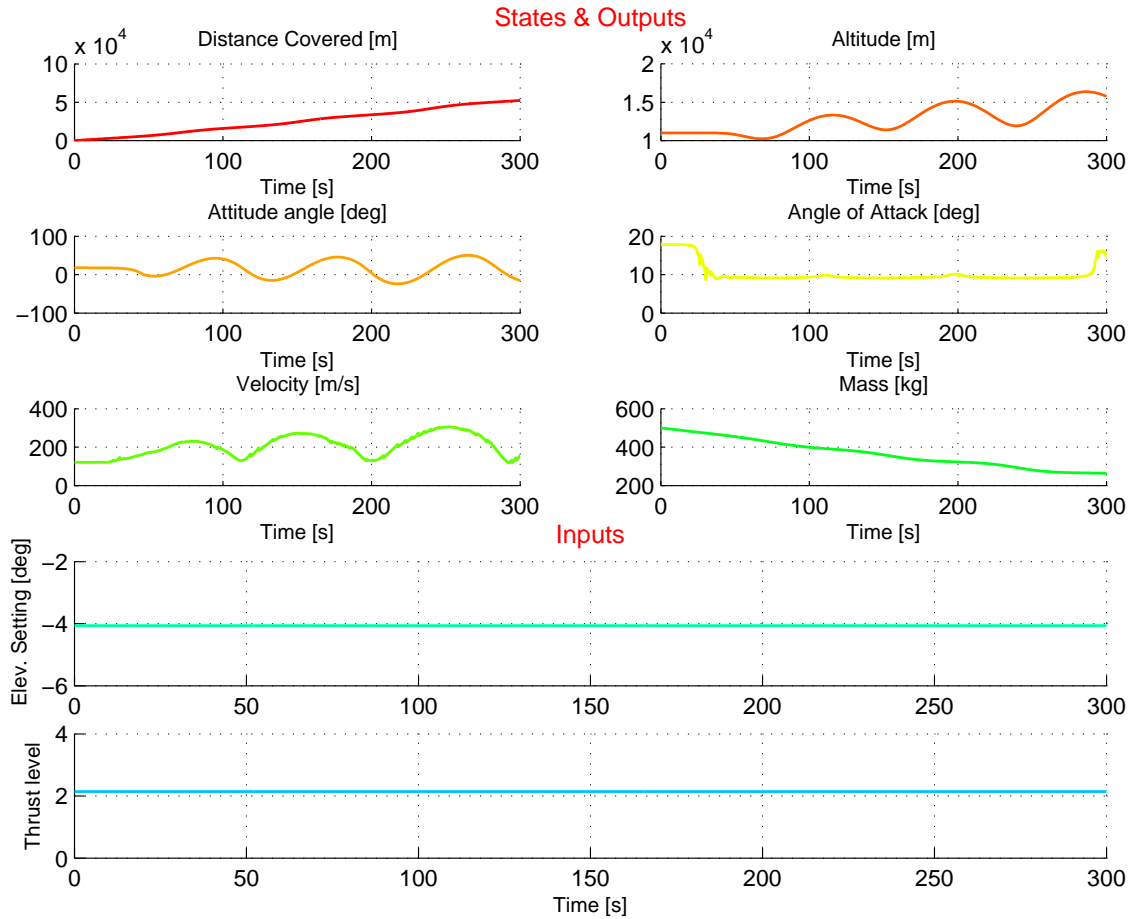


Figure 4.4: Simulation outcome for constant  $\delta_\epsilon, \delta_p$

As we can see, in the beginning (first 50s) aircraft keeps a constant altitude as well as the other properties, but as the mass decreases, the aircraft starts raising and velocity and attitude start oscillating. The linear stability analysis did not predict any divergence from the equilibrium point, because the loss of mass was not included in the model.

An interesting point to make is that when the simulation is run with an unacceptable cg position (e.g 10.3m) the altitude starts oscillating with increasing magnitude (see fig.4.5) an indicator of unstable system behavior. If the xcg increases even more, the time integration algorithm cannot find a valid solution after a certain time.

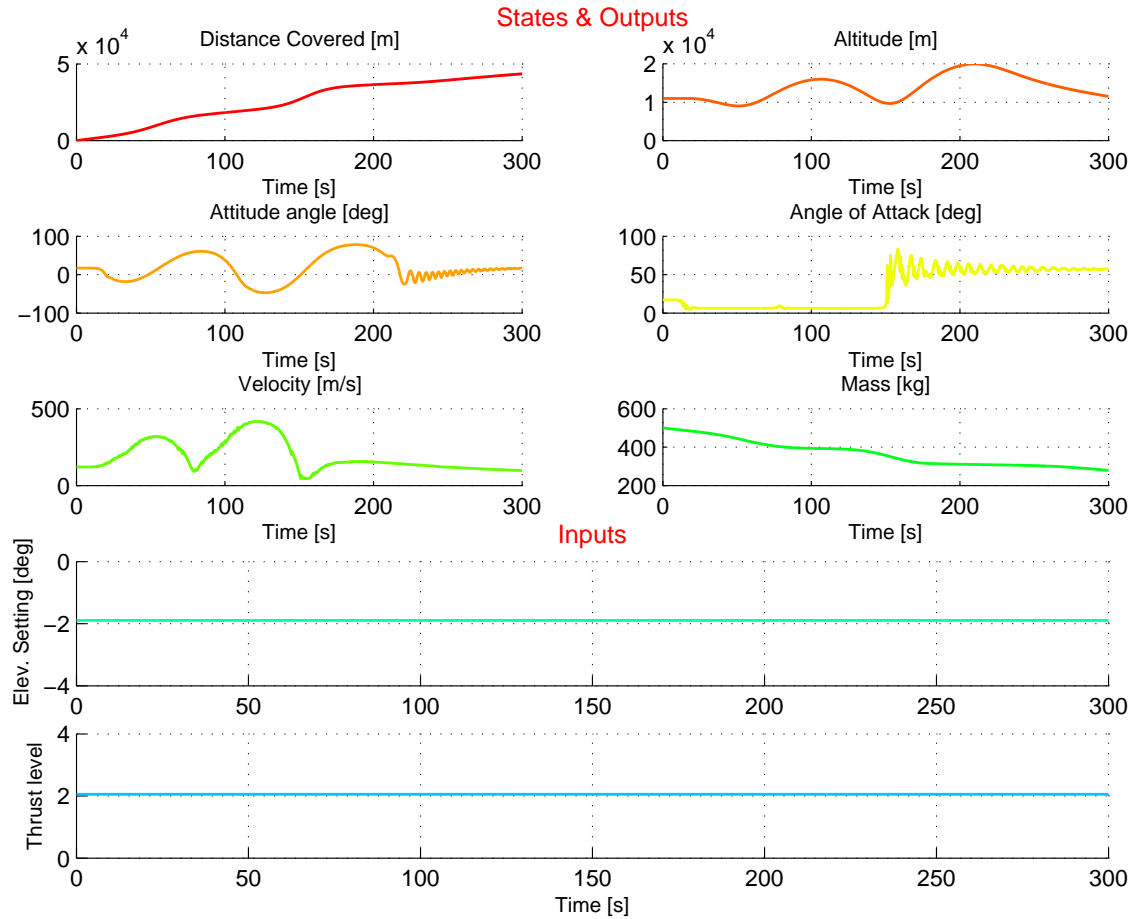


Figure 4.5: Nonlinear Simulation results for  $x_{cg} = 10.3\text{m}$

#### 4.3.1 Looping

The looping maneuver is performed by applying a negative elevator ( $5 - 6^\circ$ ) angle while having maximum thrust level. In this way the aircraft starts raising in a curved trajectory until it reaches a maximum in an upside position. Then maintaining the same elevator angle, after surpassing the max point of the flight trajectory, we increase the thrust level so that when we reach the initial altitude, we can maintain it in an equilibrium condition.<sup>9</sup> The attempt of a loop maneuver is given in fig. 4.6a-4.6b

<sup>9</sup>The elevator, thrust inputs are given in their respective csv files, handed with the code

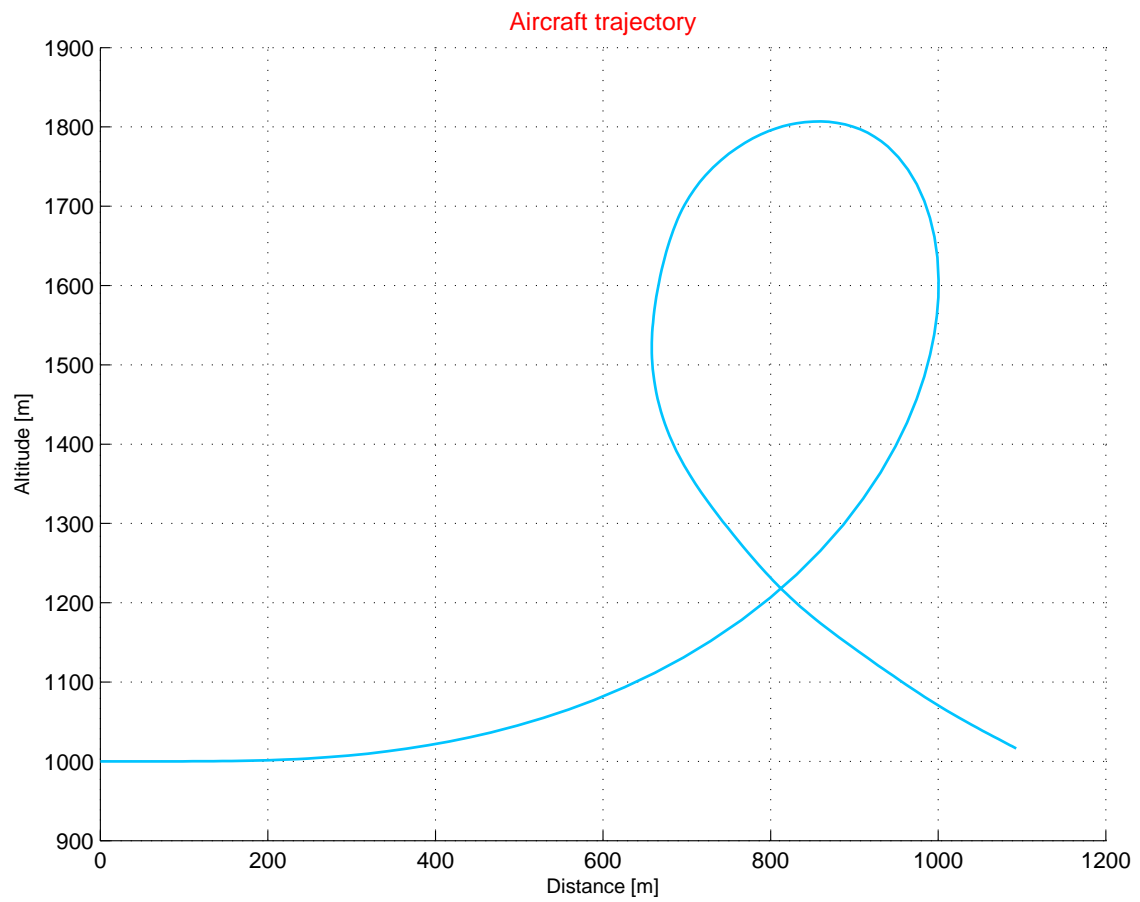


Figure 4.6: Looping Trajectory



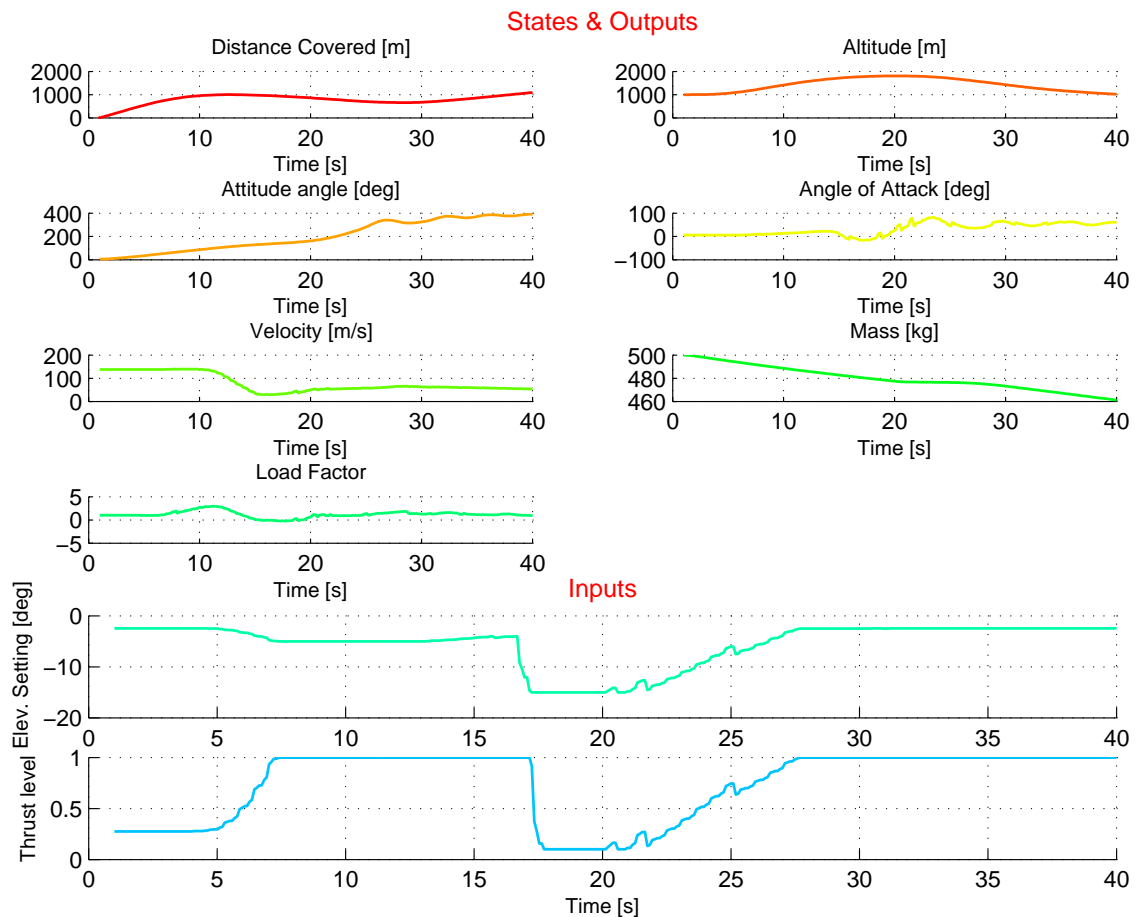


Figure 4.7: Parameters status during looping

### 4.3.2 Cobra Maneuver

### 4.3.3 The superstall

## 5 Appendix

Below are the results of the eigenvalue analysis. For each altitude and the minimum and maximum mach number each time the eigenvalues, the corresponding eigenvectors, the oscillation frequencies and the double/half time are presented.

../Project3/logfiles/eigenvalue\_analysis.log

```
*****
** Altitude = 0 m**
** Mach = 0.10 **
```

---

1. Eigenvalue =  $-0.14368 + 0.79321i$

---

Frequency = 0.1262 Hz  
Corresponding Eigenvector:  
0.890255  
-0.259188  
0.007383  
-0.028991

Time to half: 4.824131 s

---

2. Eigenvalue =  $-0.14368 - 0.79321i$

---

Frequency = 0.1262 Hz

Corresponding Eigenvector :

0.890255  
-0.259188  
0.007383  
-0.028991

Time to half: 4.824131 s

---

3. Eigenvalue =  $-0.090499+0.13136i$

---

Frequency = 0.0209 Hz

Corresponding Eigenvector :

0.366311  
0.930174  
0.002616  
-0.009383

Time to half: 7.659181 s

---

4. Eigenvalue =  $-0.090499-0.13136i$

---

Frequency = 0.0209 Hz

Corresponding Eigenvector :

0.366311  
0.930174  
0.002616  
-0.009383

Time to half: 7.659181 s

\*\*\*\*\*

\*\*\*\*\*

\*\* Altitude = 0 m\*\*

\*\* Mach = 0.66 \*\*

---

1. Eigenvalue =  $-1.7165+3.6452i$

---

Frequency = 0.5802 Hz

Corresponding Eigenvector :

-0.037312  
0.999127  
-0.000670  
0.003810

Time to half: 0.403815 s

---

2. Eigenvalue =  $-1.7165-3.6452i$

---

Frequency = 0.5802 Hz

Corresponding Eigenvector :

-0.037312  
0.999127  
-0.000670  
0.003810

Time to half: 0.403815 s

---

3. Eigenvalue =  $-0.0082273+0.056856i$

---

Frequency = 0.0090 Hz

Corresponding Eigenvector :

0.999300  
0.036945  
0.000337  
-0.000902

Time to half: 84.249725 s

---

4. Eigenvalue =  $-0.0082273-0.056856i$

---

Frequency = 0.0090 Hz

Corresponding Eigenvector :

0.999300  
0.036945  
0.000337  
-0.000902

Time to half: 84.249725 s

\*\*\*\*\*

```

*****
** Altitude = 5000 m**
** Mach = 0.10 **

```

---

1. Eigenvalue =  $-0.10482+0.081428i$

---

Frequency = 0.0130 Hz  
Corresponding Eigenvector:  
 $-0.833642$   
 $0.551061$   
 $-0.001381$   
 $0.017139$   
Time to half: 6.612794 s

---

2. Eigenvalue =  $-0.10482-0.081428i$

---

Frequency = 0.0130 Hz  
Corresponding Eigenvector:  
 $-0.833642$   
 $0.551061$   
 $-0.001381$   
 $0.017139$   
Time to half: 6.612794 s

---

3. Eigenvalue =  $0.091845+0.10436i$

---

Frequency = 0.0166 Hz  
Corresponding Eigenvector:  
 $0.298327$   
 $0.888202$   
 $0.000654$   
 $-0.001179$   
Time to double: 7.546896 s

---

4. Eigenvalue =  $0.091845-0.10436i$

---

Frequency = 0.0166 Hz  
Corresponding Eigenvector:  
 $0.298327$   
 $0.888202$   
 $0.000654$   
 $-0.001179$   
Time to double: 7.546896 s

```

*****

```

```

*****
** Altitude = 5000 m**
** Mach = 0.66 **

```

---

1. Eigenvalue =  $-0.97162+2.6963i$

---

Frequency = 0.4291 Hz  
Corresponding Eigenvector:  
 $-0.066518$   
 $0.997680$   
 $-0.000406$   
 $0.004297$   
Time to half: 0.713396 s

---

2. Eigenvalue =  $-0.97162-2.6963i$

---

Frequency = 0.4291 Hz  
Corresponding Eigenvector:  
 $-0.066518$   
 $0.997680$   
 $-0.000406$   
 $0.004297$   
Time to half: 0.713396 s

---

3. Eigenvalue =  $-0.004833+0.062448i$

---

Frequency = 0.0099 Hz  
Corresponding Eigenvector:

```

0.997963
0.063470
0.000400
-0.000578
Time to half: 143.420539 s

```

---

```

4. Eigenvalue = -0.004833-0.062448 i

```

---

```

Frequency = 0.0099 Hz
Corresponding Eigenvector:
0.997963
0.063470
0.000400
-0.000578
Time to half: 143.420539 s
*****

*****
** Altitude = 10000 m**
** Mach = 0.24 **

```

---

```

1. Eigenvalue = -1.2177

```

---

```

Frequency = 0.0000 Hz
Corresponding Eigenvector:
-0.465464
0.884820
-0.016163
0.013273
Time to half: 0.569235 s

```

---

```

2. Eigenvalue = 0.99286

```

---

```

Frequency = 0.0000 Hz
Corresponding Eigenvector:
-0.711288
0.702632
0.013685
0.013784
Time to double: 0.698128 s

```

---

```

3. Eigenvalue = -0.058837+0.14745 i

```

---

```

Frequency = 0.0235 Hz
Corresponding Eigenvector:
0.794193
0.606749
0.002573
-0.005610
Time to half: 11.780877 s

```

---

```

4. Eigenvalue = -0.058837-0.14745 i

```

---

```

Frequency = 0.0235 Hz
Corresponding Eigenvector:
0.794193
0.606749
0.002573
-0.005610
Time to half: 11.780877 s
*****

*****
** Altitude = 10000 m**
** Mach = 0.66 **

```

---

```

1. Eigenvalue = -0.52705+2.1551 i

```

---

```

Frequency = 0.3430 Hz
Corresponding Eigenvector:
-0.119907
0.992112
-0.000088

```

```

0.004829
Time to half: 1.315133 s
-----
2. Eigenvalue = -0.52705-2.1551i
-----
Frequency = 0.3430 Hz
Corresponding Eigenvector:
-0.119907
0.992112
-0.000088
0.004829
Time to half: 1.315133 s
-----
3. Eigenvalue = -0.0047843+0.068217i
-----
Frequency = 0.0109 Hz
Corresponding Eigenvector:
0.992213
0.124349
0.000477
-0.000580
Time to half: 144.879349 s
-----
4. Eigenvalue = -0.0047843-0.068217i
-----
Frequency = 0.0109 Hz
Corresponding Eigenvector:
0.992213
0.124349
0.000477
-0.000580
Time to half: 144.879349 s
*****

```

## References

- [1] Robert Dorr, Rene Francillon, and Jay Miller. *Aerofax Minigraph 12, Saab J35 Draken*. Aerofax Inc., 1987.
- [2] Bernanrd Etkin. *Dynamics of Atmospheric Flight*. John Wiley & Sons, Inc, Toronto, Canada, 1972. 00000.
- [3] HW. Rise of the Draken < HistoricWings.com :: A Magazine for Aviators, Pilots and Adventurers. 00000.